ACS APPLIED MATERIALS & INTERFACES

Research Article

www.acsami.org

Fe_3O_4/PVIM-Ni^{2+} Magnetic Composite Microspheres for Highly Specific Separation of Histidine-Rich Proteins

Yuting Zhang, Dian Li, Meng Yu, Wanfu Ma, Jia Guo, and Changchun Wang*

State Key Laboratory of Molecular Engineering of Polymers, Department of Macromolecular Science, and Laboratory of Advanced Materials, Fudan University, Shanghai 200433, China

Supporting Information

ABSTRACT: Integration of the advantages of immobilized metal-ion affinity chromatography (IMAC) and magnetic microspheres is considered as an ideal pathway for quick and convenient separation of his-tagged proteins, but rare reports concern the natural histidine-rich proteins. In this article, a novel route was presented to fabricate magnetic microspheres composed of a high-magnetic-response magnetic supraparticle (Fe_3O_4) core and a Ni^{2+}-immobilized cross-linked polyvinyl imidazole (PVIM) shell via reflux-precipitation polymerization. The unique as-prepared Fe_3O_4/PVIM-Ni^{2+} microspheres possessed uniform flower-like structure, high magnetic responsiveness, abundant binding sites, and very easy synthesis process. Taking advantage of the pure PVIM-Ni^{2+} interface and high Ni^{2+} loading amount, the microspheres exhibited remarkable selectivity, excellent sensitivity, large enrichment capacity, and high recyclability in immobilization and separation of his-tagged recombinant proteins. More interestingly, it was found that the Fe_3O_4/PVIM-Ni^{2+} microspheres also showed excellent performance for removal of the natural histidine-rich bovine serum albumin (BSA) from the complex real sample of fetal bovine serum due to the exposed histidine residues. Considering their multiple merits, this new type of Fe_3O_4/PVIM-Ni^{2+} nanomaterial displays great potential in enriching low-abundant his-tagged proteins or removing high-abundant histidine-rich natural proteins for proteomic analysis.

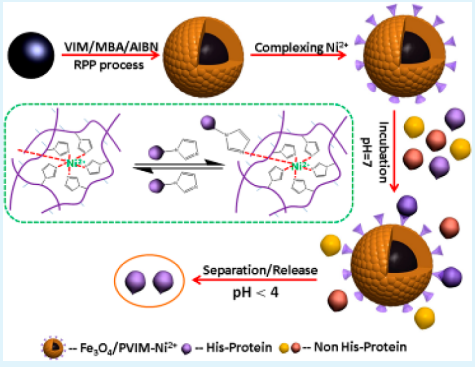

KEYWORDS: *Fe_3O_4/PVIM-Ni^{2+} core/shell microspheres, affinity ligand, selective enrichment, histidine-rich protein, BSA, removal*

1. INTRODUCTION

Over the past decade, magnetic composite microspheres have gained immense scientific and technological interest owning to their unique magnetic responsiveness and a wide range of applications in biomedical area such as protein purification,[1−3] targeted drug delivery,[4−6] cell separation,[7−9] and medical diagnosis.[10−12] The magnetic susceptibility of these microspheres allows them to be easily manipulated by applying an external magnetic field. As a major part of the magnetic composite microspheres, core/shell magnetic polymeric microspheres with tailored functional polymer shell have attracted much attention due to their high density of surface functional groups and easy modification nature. To date, the emulsion polymerization[13−15] and distillation precipitation polymerization[16,17] are among the most common methods used at present for encapsulation of polymer shell and formation of the core/shell structure. However, the former is time-consuming, and the latter has a low reaction yield. Very recently, as a great advance, reflux-precipitation polymerization[18] has been developed for improving the reaction yield and shows more advantages in preparation of core/shell microspheres with polymer shell. The continuous polymer shell provides abundant functional groups, which are essential to their applications, such as protein separation.

In protein engineering, his-tagged recombinant proteins are widely employed and the purification of them is of great importance.[19] Besides, the low-abundant biomarkers are always submerged by the high-abundant histidine-rich proteins in biomedical analysis; thus, the removal of histidine-rich proteins such as BSA or BHb prior to analysis plays a crucial role in the discovery of biomarkers. Among the various separation strategies, immobilized metal affinity chromatography (IMAC)[20] is a versatile method for the selective and reliable separation of his-tagged proteins, which relies on the interaction between an immobilized metal ion and electron donor groups such as histidine located on the surface of proteins. To integrate the advantages of magnetic nanoparticles and IMAC should be a powerful technique for his-tagged protein separation, and much attentions have been paid to this area in the past few years.[21−28] Nitrilotriacetic acid (NTA)[29] and iminodiacetic acid (IDA)[30] are the most common affinity ligands used for immobilizing Ni^{2+} and then applied to isolate his-tagged protein. For example, Xu and co-workers reported nickel-nitrilotriacetic acid (Ni-NTA)-terminated MNPs for selective binding to his-tagged proteins.[31,32] However, the ligand NTA is expensive and inconvenient to obtain. Zhang et al. synthesized Fe_3O_4 particles immobilized with iminodiacetic acid (IDA) charged by Cu^{2+} or Ni^{2+} ions as IMAC adsorbents

Received: March 18, 2014
Accepted: April 25, 2014
Published: April 25, 2014

for selective capture of histidine-rich bovine hemoglobin (BHb).[33,34] While the synthetic steps were complicated and the IDA was post-grafted onto the microspheres with low density of the functional groups. To date, no other ligands for chelating Ni^{2+} were reported, and the currently existing ligands NTA or IDA failed to form a continuous shell for high metal-ion density. Therefore, the invention of a novel robust ligand that can generate a continuous shell and high loading density of metal-ion on the magnetic microspheres is of great significance.

Herein, in order to develop a new kind of magnetic microspheres for immobilizing Ni^{2+}, poly(vinyl imidazole) was firstly encapsulated as a polymer shell onto the magnetic core by reflux-precipitation polymerization (Fe_3O_4/PVIM). After abundant Ni^{2+} were immobilized on the surface, the composite microspheres (Fe_3O_4/PVIM-Ni^{2+}) were employed to separate not only his-tagged recombinant protein but also natural histidine-rich protein such as BSA or BHb. The well-designed magnetic microspheres possess the following attractive advantages: (1) The poly(vinyl imidazole) shell could be coated onto magnetic core with desirable morphology and structure through reflux-precipitation polymerization with only 10 min, the polymerization process was robust and facile. (2) The poly(vinyl imidazole) shell furnished highly pure interfaces with imidazole metal complexes, which greatly improves the enrichment specificity and sensitivity towards his-tagged or histidine-rich proteins. (3) The rough poly(vinyl imidazole) shell offered abundant binding sites for Ni^{2+}, leading to a large enrichment capacity for targeting proteins (284 mg his-tagged recombinant protein/g of beads and 240 mg histidine-rich protein BSA/g of beads). (4) The reversible adsorption and desorption are easy to implement, ensuring high recovery and excellent recyclability (more than 7 times). (5) A high-magnetic-response Fe_3O_4 core allows easy separation by simply using an external magnet (less than 20 s). The experimental results also demonstrated the excellent performance of these Fe_3O_4/PVIM-Ni^{2+} microspheres in separation of histidine-rich natural proteins from real biological systems, showing great potential in further practical applications.

2. EXPERIMENTAL SECTION

2.1. Materials. Iron(III) chloride hexahydrate ($FeCl_3 \cdot 6H_2O$), ammonium acetate (NH_4Ac), ethylene glycol (EG), anhydrous ethanol, trisodium citrate dihydrate, nickel chloride hexahydrate ($NiCl_2 \cdot 6H_2O$), aqueous ammonia solution (25%), and acetic acid (HAc) were purchased from Shanghai Chemical Reagents Company and used as received. γ-Methacryloxypropyltrimethoxy-silane (MPS) was bought from Jiangsu Chen Guang Silane Coupling Reagent Co., Ltd. N,N′-methylenebis(acrylamide) (MBA) was obtained from Fluka and recrystallized from acetone. 2,2-azobis(isobutyronitrile) (AIBN) was supplied by Sinopharm Chemical Reagents Company and recrystallized from ethanol. 1-Vinylimidazole (VIM) was purchased from Aladdin. Cytochrome c (Cyt C, 95%), Myoglobin (MYO, 95%), horseradish peroxidase (HRP, 98%), bovine hemoglobin (BHb, 95%), and bovine serum albumin (BSA, 95%) were purchased from Sigma-Aldrich. His-tagged protein Trx-His × 6-DDDDK (EK site)-Protein S100A13 was provided by Novoprotein Scientific Incorporation. Deionized water (18.4 MΩ cm) used for all experiments was obtained from a Milli-Q system (Millipore, Bedford, MA).

2.2. Synthesis of Fe_3O_4/MPS. Fe_3O_4 magnetic supraparticles (MSPs) were prepared by a modified solvothermal reaction similar to our previous work.[35,36] Typically, 1.350 g of $FeCl_3 \cdot 6H_2O$, 3.854 g of NH_4Ac, and 0.4 g of sodium citrate were dissolved in 70 mL ethylene glycol. The mixture was stirred vigorously for 1 h at 170 °C to form a homogeneous black solution and then transferred into a 100 mL Teflon-lined stainless-steel autoclave. The autoclave was heated to 200 °C and maintained for 16 h. Then, it was cooled to room temperature. The black product was washed with ethanol several times, collected with a magnet, and then re-dispersed in ethanol for subsequent use.

Modification of MSPs with γ-methacryloxypropyltrimethoxy-silane (MPS) to form abundant double bonds on the surface was achieved as follows: 40 mL of ethanol, 10 mL of deionized water, 1.5 mL of $NH_3 \cdot H_2O$, and 0.6 g of MPS were added into 0.3 g of Fe_3O_4; then, the mixture was vigorously stirred for 24 h at 70 °C. The obtained product was separated by a magnet and washed with ethanol to remove excess MPS. The resultant Fe_3O_4/MPS microspheres were dried in a vacuum oven at 40 °C until a constant weight was reached.

2.3. Preparation of Fe_3O_4/PVIM Core/Shell Composite Microspheres by RPP Method. The core/shell Fe_3O_4/PVIM microspheres were synthesized by a facile reflux-precipitation polymerization (RPP) of VIM, with MBA as the cross-linker and AIBN as the initiator, in acetonitrile. Specifically, 100 mg of Fe_3O_4/MPS seed microspheres was dispersed in 80 mL acetonitrile in a dried 150 mL single-necked flask under ultrasonic condition for 2 min. Then, a mixture of 400 mg of VIM, 100 mg of MBA, and 10 mg of AIBN was added to the flask to initiate the polymerization. The reaction mixture was heated from ambient temperature to the boiling state within 20 min and maintained at 110 °C for 10 min. The obtained Fe_3O_4/PVIM microspheres were collected by a magnet and washed with ethanol and water several times in order to eliminate excess reactants and a few generated polymer microspheres.

2.4. Fabrication of Fe_3O_4/PVIM-Ni^{2+} Microspheres. Fe_3O_4/PVIM (50 mg) was added to 20 mL $NiCl_2 \cdot 6H_2O$ solution (0.1 M) and stirred for 0.5 h at room temperature. The product was separated by magnet from the solution and washed for several times with water. The resultant Fe_3O_4/PVIM-Ni^{2+} microspheres were dried in a vacuum oven at 40 °C and stored for further use.

2.5. His-tagged Recombinant Protein or Natural Histidine-rich Protein Binding and Separation. The obtained Fe_3O_4/PVIM-Ni^{2+} magnetic microspheres were first washed with ethanol for three times and then suspended in deionized water (10 mg/mL). A mixture of 5 μg Cyt c, 5 μg his-tagged protein, and 5 μg HRP was dissolved in 100 μL deionized water; then, 1 mg Fe_3O_4/PVIM-Ni^{2+} was added and incubated at room temperature for 20 min with shaking. After magnetic separation, the supernatant was removed, and the protein-bonded composite microspheres were washed twice with deionized water to remove the non-specifically adsorbed proteins. Subsequently, the trapped his-tagged or histidine-rich proteins were directly eluted from the microspheres with 50 μL HAc. The enrichment of his-tagged protein from the complex sample *E. coli* lysate (2 μL) has the same procedure as that for the model proteins. The protein solutions in each step (including the stock, supernatant and elute solutions) were all collected and lyophilized for SDS-PAGE analyses.

2.6. Removal of BSA from Fetal Bovine Serum. The enrichment of BSA from real biological samples (fetal bovine serum) has the similar procedure as that for the model proteins, just exchanging the mixed proteins with the fetal bovine serum (1 μL). The materials used are Fe_3O_4/PVIM-Ni^{2+} and Fe_3O_4/PMG-IDA-Ni^{2+}, respectively. The protein solutions in each step (including the stock, supernatant, and elute solutions) were all collected and lyophilized for SDS-PAGE analyses, and the results of the two types of materials were compared.

2.7. Testing the Sensitivity of Fe_3O_4/PVIM-Ni^{2+} toward His-tagged Protein and Histidine-rich Protein BSA. The obtained Fe_3O_4/PVIM-Ni^{2+} magnetic microspheres were first washed with ethanol for three times and then suspended in deionized water (10 mg/mL). His-tagged protein (4 μg) or histidine-rich protein BSA (4 μg) was dissolved in 1 mL, 2 mL, and 4 mL deionized water, respectively; then, 1 mg Fe_3O_4/PVIM-Ni^{2+} was added and incubated at room temperature for 20 min with shaking. After magnetic separation, the supernatant was removed, and the protein-bonded composite microspheres were washed twice with deionized water. Subsequently, the trapped his-tagged protein or histidine-rich protein BSA was directly eluted from the microspheres with 10 μL HAc. The protein solutions (10 μL) in each step (including the stock and elute solutions) were all collected and lyophilized for SDS-PAGE analyses.

2.8. Investigating the Recyclability of Fe_3O_4/PVIM-Ni^{2+} towards His-tagged Protein and Histidine-rich Protein BSA. The obtained Fe_3O_4/PVIM-Ni^{2+} magnetic microspheres were first washed with ethanol three times and then suspended in deionized water (10 mg/mL). His-tagged protein (5 μg) or BSA (5 μg) was dissolved in 100 μL deionized water respectively; then, 1 mg Fe_3O_4/PVIM-Ni^{2+} was added and incubated at room temperature for 20 min with shaking. After washing for twice with deionized water, the trapped his-tagged protein or histidine-rich protein BSA was directly eluted from the microspheres with 50 μL HAc. Then, the microspheres were chelated with $NiCl_2 \cdot 6H_2O$ for another 5 min and used for the separation experiment again. The total experimental process was repeated for seven times, and the eluate in each step was collected and lyophilized for SDS-PAGE analyses.

2.9. Characterization. High-resolution transmission electron microscopy (HR-TEM) images were taken on a JEM-2100F transmission electron microscope at an accelerating voltage of 200 kV. Samples dispersed at an appropriate concentration were cast onto a carbon-coated copper grid. Field-emission scanning electron microscopy (FE-SEM) was performed on a Hitachi S-4800 scanning electron microscope at an accelerating voltage of 20 kV. Sample dispersed at an appropriate concentration was cast onto a glass sheet at room temperature and sputter-coated with gold. Hydrodynamic diameter (Dh) measurements were conducted by dynamic light scattering (DLS) with a ZEN3600 (Malvern, UK) Nano ZS instrument using He−Ne laser at a wavelength of 632.8 nm. Fourier transform infrared spectra (FT-IR) were recorded on a Magna-550 (Nicolet, U.S.A.) spectrometer. Spectra were scanned over the range 400−4000 cm^{-1}. All of the dried samples were mixed with KBr and then compressed to form pellets. Powder X-ray diffraction (XRD) patterns were obtained using a X'Pert Pro (Panalytical, Netherlands) diffraction meter with Cu Kα radiation at λ = 0.154 nm operating at 40 kV and 40 mA. Thermogravimetric analysis (TGA) measurements were performed on a Pyris 1 TGA instrument. All measurements were taken under a constant flow of nitrogen of 40 mL/min. The temperature was first increased from room temperature to 100 °C and held until constant weight, and then, it was increased from 100 to 800 °C at a rate of 20 °C/min. Magnetic characterization was carried out on a VSM on a Model 6000 physical property measurement system (Quantum, U.S.A.) at 300 K. X-ray photoelectron spectrum (XPS) was conducted using an RBD upgraded PHI-5000C (PerkinElmer, U.S.A.) ESCA system with Mg Kα radiation ($h\nu$ = 1253.6 eV) at 250 W and 14.0 kV with a detection angle at 54°. Inductively coupled plasma-atomic emission spectrometry (ICP-AES) measurement was taken on a P-4010 instrument. The sodium dodecyl sulfate-polyacrylamide gel electrophoresis (SDS-PAGE) was performed using 4-15% precast polyacrylamide gels and Mini-Protean Tetra cell (Tanon, China). Protein concentration was obtained by measuring absorbance at 284 nm using BioTek Power Wave XS2 microplate reader.

3. RESULTS AND DISCUSSION

The procedure for the fabrication of composite microspheres containing a superparamagnetic core and a functional polymer shell with abundant Ni^{2+} was schematically illustrated in Scheme 1. Firstly, Fe_3O_4 (about 200 nm) cores were prepared by a modified solvothermal reaction; secondly, silane coupling agent MPS was employed to modify the MSPs with abundant available double bonds, which promotes the polymer coating in the next step; thirdly, a flower-like layer of PVIM was coated onto the Fe_3O_4/MPS surface by reflux-precipitation polymerization (RPP) of VIM (monomer) and MBA (cross-linker) to form Fe_3O_4/PVIM core/shell microspheres; finally, $NiCl_2 \cdot 6H_2O$ solution was added to immobilize Ni^{2+} on the surface of the microspheres, which provides abundant binding sites for histidine-rich proteins. The vinyl imidazole as a novel functional monomer was polymerized and coated on the magnetic core with such a short time for the first time.

Scheme 1. Schematic Illustration of the Fabrication Procedures of Fe_3O_4/PVIM-Ni^{2+} Microspheres and Their Application in Selective Enrichment or Removal of Histidine-rich Protein

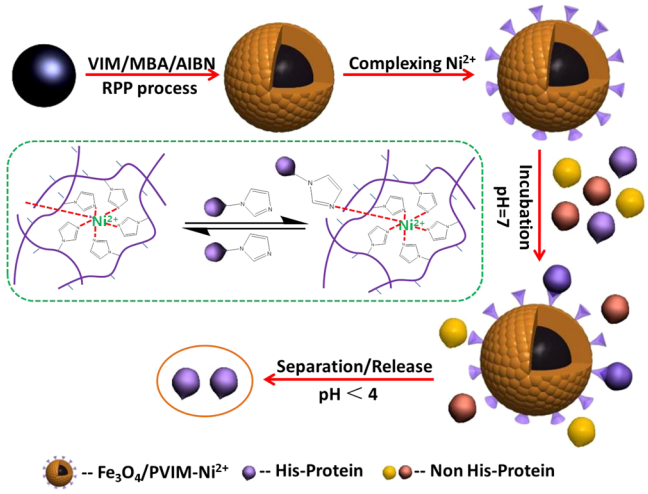

Moreover, the poly(vinyl imidazole) was firstly used as a shell for binding of Ni^{2+}, other than traditionally employed NTA or IDA ligand, providing a new method for separating histidine-rich proteins.

3.1. Preparation of Magnetic Core/Shell Fe_3O_4/PVIM Microspheres by RPP Method. Fe_3O_4/MPS was prepared similar to our previous report.[36] Then, cross-linked PVIM shell was coated on Fe_3O_4/MPS by reflux-precipitation polymerization, which is a novel and convenient polymerization process.[18] As PVIM species are not soluble in acetonitrile, the generated PVIM oligomers will continuously precipitate from the solution to the surface of Fe_3O_4/MPS, and gradually forming a functional polymer shell. Since the monomer VIM has a very high reactivity, the polymerizing and encapsulating process finished in only 10 min and the uniform flower-like microspheres were obtained. Compared with the traditional emulsion polymerization, it saves a lot of time and offers a brand-new effective method for the encapsulation of PVIM.

Transmission electron microscope (TEM) images of Fe_3O_4 and Fe_3O_4/PVIM core/shell microspheres are shown in Figure 1. The magnetic cores of Fe_3O_4 had an average diameter of about 200 nm and were uniform both in shape and in size. After coated with PVIM, they showed obvious flower-like core/shell structure. When the crosslinking degree is as low as 10%, the shell only has poor structural integrity (Figure 1b) due to the low precipitation ability of PVIM. When the crosslinking degree is higher than 20%, the polymeric shell became integrated and the flower-like surface remained. The scanning electron microscope (SEM) image (Supporting Information Figure S1a) indicated that the magnetic clusters were composed of many small nanocrystals, which were in consistence with the previous literature.[36] After being coated with a PVIM shell, the composite microspheres had a rougher flower-like polymer shell (Supporting Information Figure S1b). X-ray diffraction (XRD) measurement (Figure 3a) was employed to determine the property of MSPs. All the diffraction peaks in the XRD patterns were indexed and assigned to the typical cubic structure of Fe_3O_4 (JCPDS 75-1609, Supporting Information Figure S2). Meanwhile, the crystallinity of Fe_3O_4 remained very well (Figure 3a(ii)). The hydrodynamic diameter and size

dx.doi.org/10.1021/am501626t | ACS Appl. Mater. Interfaces 2014, 6, 8836−8844

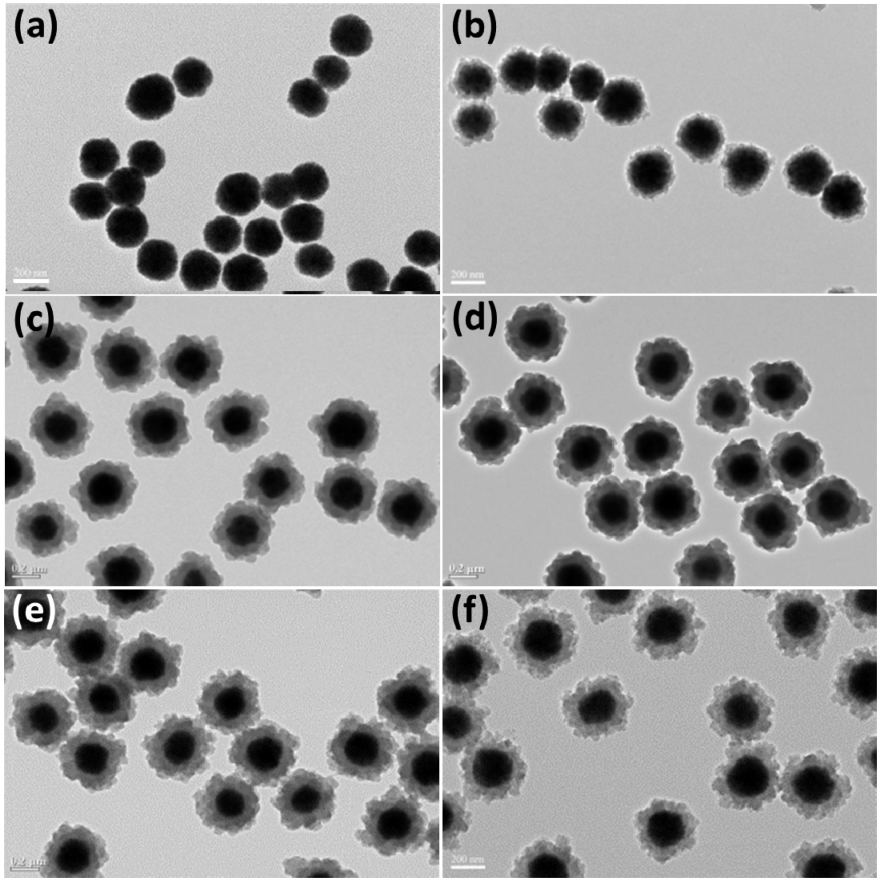

Figure 1. TEM images of (a) Fe_3O_4/MPS, (b) Fe_3O_4/PVIM-1, (c) Fe_3O_4/PVIM-2, (d) Fe_3O_4/ PVIM-3, (e) Fe_3O_4/PVIM-4, and (f) Fe_3O_4/PVIM-5. The scale bars are all 200 nm.

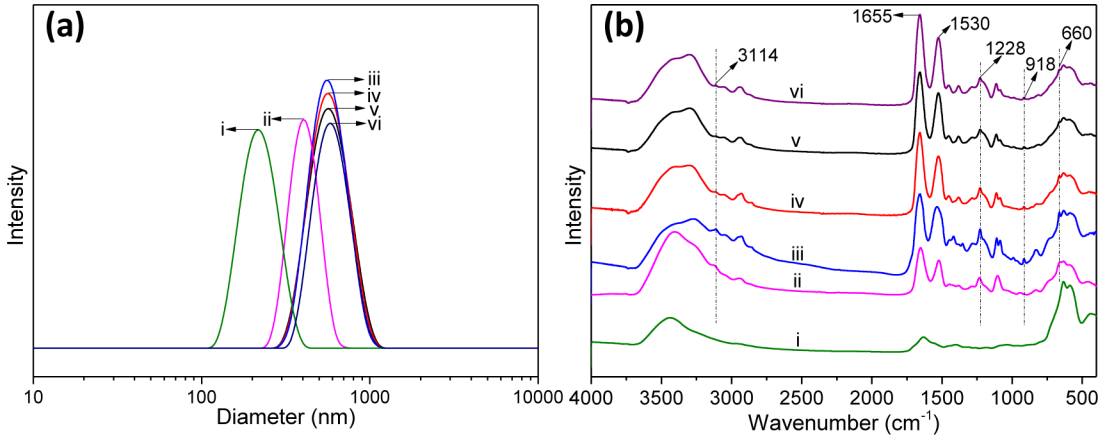

Figure 2. (a) DLS curves and (b) FT-IR spectra of (i) Fe_3O_4/MPS, (ii) Fe_3O_4/PVIM-1, (iii) Fe_3O_4/PVIM-2, (iv) Fe_3O_4/PVIM-3, (v) Fe_3O_4/PVIM-4, and (vi) Fe_3O_4/PVIM-5.

distribution were determined by dynamic light scattering (DLS). The hydrodynamic diameter (D_h) of Fe_3O_4 was about 300 nm (Figure 2a), which was close to the size measured by TEM. After encapsulation, the D_h of Fe_3O_4/PVIM increased to 513 nm, which was much larger than the size from TEM due to the good hydrophilicity. The dispersion of Fe_3O_4/PVIM was demonstrated to have an excellent stability, which facilitated its further chelation of Ni^{2+} in water. The size and polydispersity indexes (PDI) of Fe_3O_4 and different shell crosslinking degree of Fe_3O_4/PVIM are summarized in Table 1, indicating that all the particles are nearly uniform.

The functional group density on the surface can be tuned by changing the feeding ratio of VIM and MBA. We kept the total weight constant (500 mg), and the ratio of VIM and MBA varied from 9:1, 4:1, 3:2, 2:3, to 1:4. FT-IR spectra were employed to monitor the changing trend of cross-linker amount in the polymer shell. As shown in Figure 2b, the peak at 584 cm^{-1} appearing in all curves was attributed to the typical stretching vibration modes of Fe−O in Fe_3O_4. The new peaks at 3114, 1228, 918, and 660 cm^{-1} in Figure 2b(ii−vi) were attributed to the vibrations of imidazole ring of VIM, and the peaks at 1655 cm^{-1} and 1530 cm^{-1} reflected the vibrations

dx.doi.org/10.1021/am501626t | ACS Appl. Mater. Interfaces 2014, 6, 8836−8844

Table 1. Recipes and Particle Size of Fe_3O_4/PVIM with Different Crosslinking Degree

sample code	crosslinking degree/%[a]	VIM/mg	MBA/mg	D_h/nm	PDI
Fe_3O_4/PVIM-1	10	450	50	411	0.049
Fe_3O_4/PVIM-2	20	400	100	513	0.016
Fe_3O_4/PVIM-3	40	300	200	525	0.070
Fe_3O_4/PVIM-4	60	200	300	574	0.076
Fe_3O_4/PVIM-5	80	100	400	588	0.134

[a]Crosslinking degree here means the theoretical crosslinking degree, which is defined as the weight ratio of cross-linker (MBA) to the whole monomer (MBA+VIM).

of C═O and N−H in MBA, which further proved the coating of cross-linked PVIM layer. Besides, when the crosslinking degree is higher than 20%, the intensity of the characteristic peak of imidazole ring from PVIM weakened gradually as the crosslinking degree increased.

3.2. Fabrication of Magnetic Fe_3O_4/PVIM-Ni^{2+} Microspheres. Nickel ion has a strong binding ability with imidazole groups, and it is rational that we can immobilize Ni^{2+} onto the surface of Fe_3O_4/PVIM and apply it to purify histidine-rich proteins. X-ray photoelectron spectroscopy (XPS) and energy dispersive X-ray (EDX) spectrum were recorded to identify the composition of the core/shell microspheres qualitatively (Supporting Information Figure S3), which proved the existence of Ni^{2+}. The amount of Ni^{2+} on the surface of the microspheres was further quantified by atomic absorption spectrum (AAS) (Table 2). From Table 2, we can find that the

Table 2. Loading Amount of Ni^{2+} in Different Samples of Fe_3O_4/PVIM-Ni^{2+}

sample code	Ni^{2+} loading amount (mg/g)
Fe_3O_4/PVIM-1-Ni^{2+}	11
Fe_3O_4/PVIM-2-Ni^{2+}	55
Fe_3O_4/PVIM-3-Ni^{2+}	31
Fe_3O_4/PVIM-4-Ni^{2+}	10
Fe_3O_4/PVIM-5-Ni^{2+}	6

chelated amount of Ni^{2+} reaches the highest when the crosslinking degree is 20%. This result can be explained as following: when the crosslinking degree is lower than 20%, the precipitation ability of the copolymer poly(VIM-*co*-MBA) is poor and only a very thin shell is formed, which contains just a low amount of imidazole groups, and the low amount of imidazole groups leads to the low loading amount of Ni^{2+}. While when the crosslinking degree is higher than 20%, a thick shell of about 80 nm is formed and the abundant imidazole groups are immobilized in the polymer shell. As the crosslinking degree further increases, the number of the imidazole group starts tail off due to the low feeding ratio of VIM; this result also agrees well with that of FT-IR spectra. Thus, the higher crosslinking degree will result in low density of imidazole group and low Ni^{2+} loading amount in the polymer shell, which is basically in accord with our expectation. Then, we chose the microspheres with a crosslinking degree of 20% for further characterization.

Thermogravimetric analysis (TGA) measurement was carried out (Figure 3b). At first, the difference between curves (i) and (ii) was attributed to the encapsulated cross-linked PVIM shell; the amount of PVIM shell was calculated to be approximate 65 wt %. Subsequently, Ni^{2+} was incorporated onto the microspheres via the chelation of Ni^{2+} with the imidazole groups for further binding with the imidazole groups of histidine-rich proteins (the complexation mechanism is illustrated in Scheme 1). Due to the fact that Ni^{2+} cannot be burned out in an N_2 atmosphere, the total mass will maintain, and it is reasonable that the weight loss will decrease a little after complexed with Ni^{2+}, as shown in Figure 3b(iii). The magnetic hysteresis curves (Figure 3c) measured by vibrating sample magnetometer (VSM) demonstrated that all the microspheres have no obvious remanence or coercivity at 300 K, indicating that they are all superparamagnetic. The saturation magnetization (Ms) value of Fe_3O_4/MPS was 67.2 emu/g. Upon the encapsulation of PVIM layer and the chelating of Ni^{2+}, the Ms value reduced to 21.4 and 19.5 emu/g, respectively. These results supplementally verified the magnetic content from TGA analysis. The magnetic responsiveness of the final product Fe_3O_4/PVIM-Ni^{2+} is strong enough to facilitate the quick separation of the composite microspheres from solution (within 20 s) using a magnet (Figure 3d). We chose the sample which chelated the largest amount of Ni^{2+} (Fe_3O_4/PVIM-2-Ni^{2+}) for the subsequent enrichment of his-tagged protein and the removal of abundant BSA in the fetal bovine serum.

3.3. Application in Separation and Enrichment of His-tagged Protein. We first tested the binding capability of Fe_3O_4/PVIM-2-Ni^{2+} for purification of his-tagged Trx-His × 6-DDDDK (EK site)-Protein S100A13Cel48F, which has a molecular weight of 25.6 kDa (229 amino acids), and the amino acid sequence is presented in the Supporting Information. Based on the enrichment process, as shown in Scheme 2, we determined the binding capacity of Fe_3O_4/PVIM-2-Ni^{2+} towards his-tagged protein to be around 284 mg/g (protein/beads) measured by a microplate reader at the wavelength of 284 nm. The protein concentration of the stock solution was 50 μg/mL (1 mL deionized water containing 50 μg his-tagged protein), and 1 mg Fe_3O_4/PVIM-2-Ni^{2+} was incubated with 500 μL stock solution. After incubation and magnetic separation, 10 μL elution solution (HAc) was applied to elute his-tagged protein from the microspheres. Then, 10 μL stock solution, 10 μL supernatant, and 10 μL eluent were collected and lyophilized for SDS-PAGE analyses. As shown in Figure 4a, the his-tagged protein concentration in the eluent was much higher than that in the stock solution by comparing the difference of the band densities on the SDS-PAGE gel, indicating that the his-tagged recombinant protein could be effectively enriched and concentrated by the magnetic microspheres from a stock solution under low concentration, which is essential for the purification of low-expressed his-tagged recombinant protein from crude *E. coli* lysate.

To further investigate the specific enrichment of his-tagged protein in a mixture of proteins with low histidine residues, a mixture of 5 μg HRP, 5 μg Cyt c and 5 μg recombinant his-tagged protein were dissolved in deionized water. The enrichment results of Fe_3O_4/PVIM-2-Ni^{2+} toward his-tagged protein are shown in Figure 4b. After enrichment with Fe_3O_4/PVIM-2-Ni^{2+}, the recombinant his-tagged protein was effectively enriched and eluted from the microspheres without non-specific adsorption of other proteins. Moreover, in order to test its selectivity in real complex samples, we used the microspheres to enrich recombinant his-tagged protein from crude *E. coli* lysate. As shown in Figure 4c, before enrichment, his-tagged protein was submerged by other proteins in the E. coli lysate, while after enrichment with Fe_3O_4/PVIM-2-Ni^{2+},

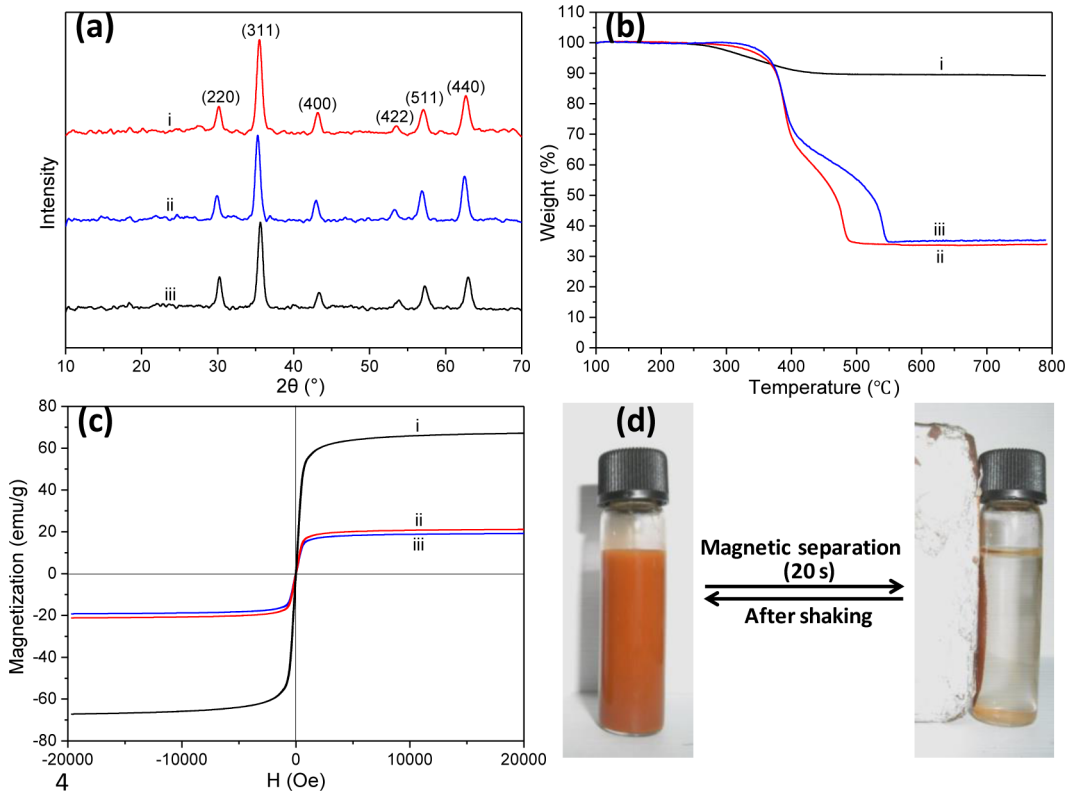

Figure 3. (a) XRD patterns, (b) TGA, and (c) VSM curves of (i) Fe_3O_4/MPS, (ii) Fe_3O_4/PVIM-2, and (iii) Fe_3O_4/PVIM-2-Ni^{2+}. (d) Magnetic separation behavior of Fe_3O_4/PVIM-2-Ni^{2+} microspheres.

Scheme 2. Schematic Illustration of the Detailed Selective Enrichment Process for the Histidine-rich Protein Using Fe_3O_4/PVIM-Ni^{2+} Microspheres

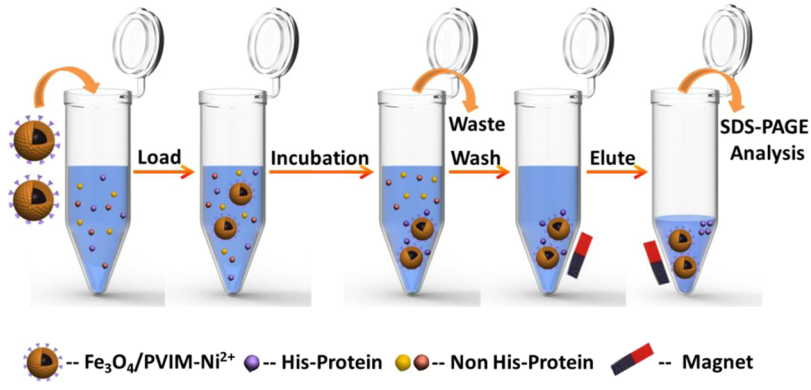

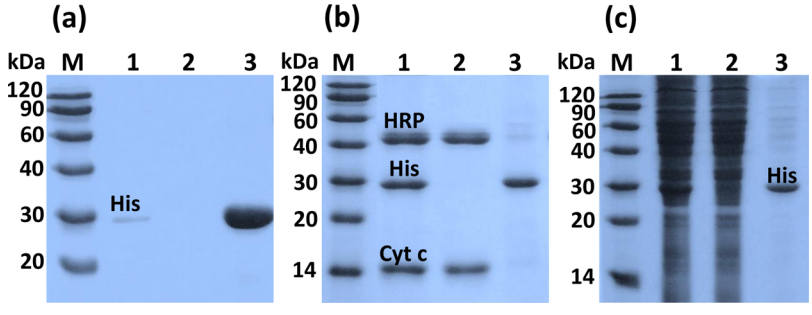

Figure 4. SDS-PAGE analysis of (a) the enrichment of pure his-tagged protein, (b) the enrichment of his-tagged protein from model proteins, (c) the enrichment of his-tagged protein from *E. coli* lysate. Lane M: the protein molecular weight marker. Lane 1: before enrichment. Lane 2: after enrichment with Fe_3O_4/PVIM-Ni^{2+}. Lane 3: eluate with acidic solution.

dx.doi.org/10.1021/am501626t | ACS Appl. Mater. Interfaces 2014, 6, 8836−8844

almost only his-tagged protein was fished out and released from the microspheres (Figure 4c, Lane 3). To further demonstrate the importance of Ni^{2+}, Fe_3O_4/PVIM-2 was used as a control for the separation of his-tagged protein from E. coli lysate, and no target protein was released from the microspheres (Supporting Information Figure S5, Lane 5). The results show that Fe_3O_4/PVIM-2-Ni^{2+} has good binding specificity toward his-tagged protein against other proteins even in the complex sample *E. coli* lysate.

3.4. Application in Separation and Enrichment of Natural Histidine-rich Protein BSA and BHb. Serum albumin and hemoglobin, as high-abundant proteins, widely existed in animal blood, and they always intervene in the detection of low-abundant biomarkers; thus, the removal of them is of great significance. BSA contains 17 histidine and BHb contains 32 histidine in their amino acid sequence (see the Supporting Information), and it is rational to remove BSA and BHb from the blood utilizing the Fe_3O_4/PVIM-2-Ni^{2+} microspheres. When mixed with the proteins of HRP and MYO, the histidine-rich proteins of BSA and BHb could be selectively fished out from the pool of mixed proteins (Figure 5a), demonstrating the excellent separation effect of Fe_3O_4/PVIM-2-Ni^{2+} toward proteins with non-adjacent histidine as well. By using a microplate reader at the wavelength of 284 nm, we determined the binding capacity of Fe_3O_4/PVIM-Ni^{2+} towards BSA to be around 240 mg/g (protein/beads).

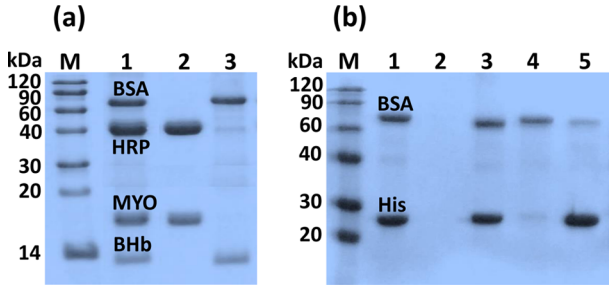

Figure 5. SDS-PAGE analysis of (a) the enrichment of histidine-rich protein BSA and BHb from model proteins. Lane M: the protein molecular weight marker. Lane 1: before treatment. Lane 2: after treatment with Fe_3O_4/PVIM-Ni^{2+}. Lane 3: eluate with acidic solution. (b) The enrichment of histidine-rich protein BSA and his-tagged protein. Lane M: is the protein molecular weight marker. Lane 1: before treatment. Lane 2: after treatment with Fe_3O_4/PVIM-Ni^{2+}. Lane 3: eluate from Fe_3O_4/PVIM-Ni^{2+}. Lane 4: after treatment with Fe_3O_4/PMG-IDA-Ni^{2+}. Lane 5: eluate from Fe_3O_4/PMG-IDA-Ni^{2+}.

In addition, it is necessary to compare the enrichment capability of Fe_3O_4/PVIM-2-Ni^{2+} with Fe_3O_4/PMG-IDA-Ni^{2+} which was reported in our previous work.[36] After enrichment using Fe_3O_4/PVIM-Ni^{2+}, the his-tagged recombinant protein and histidine-rich natural protein BSA were both separated entirely from the stock solution (Figure 5b, Lane 3). While after enrichment using Fe_3O_4/PMG-IDA-Ni^{2+}, all his-tagged recombinant protein and only a small part of BSA were separated and eluted from the microspheres (Figure 5b, Lane 5). Thus, a conclusion could be drawn that the two materials exhibited almost the same enrichment effect toward his-tagged protein, while the Fe_3O_4/PVIM-Ni^{2+} displayed much better performance in the isolation of BSA with non-adjacent histidine. This may be ascribed to the fact that Fe_3O_4/PVIM-Ni^{2+} owns a continuous shell of polyvinyl imidazole on the core, and the adjacent imidazole groups have a synergistic effect with the non-adjacent histidine in BSA, which formed a multivalent interaction to form a stable state. Thus, the BSA was immobilized onto the microspheres tightly, while the Fe_3O_4/PMG-IDA-Ni^{2+} failed to strongly interact with BSA due to the lack of the above synergistic effect.

3.5. Application of Fe_3O_4/PVIM-2-Ni^{2+} for Removing High Abundant BSA from Fetal Bovine Serum. Since the proteomics research has gained a great deal of interest, the interference of high-abundant protein such as BSA should be eradicated prior to the MS analysis. Fetal bovine serum was used as the real complex sample, Fe_3O_4/PVIM-2-Ni^{2+} and Fe_3O_4/PMG-IDA-Ni^{2+} were utilized for the separation of BSA in the serum. In Figure 6, almost all the high-abundant histidine-rich BSA was removed and eluted from the microspheres after isolation using Fe_3O_4/PVIM-2-Ni^{2+}. While after separation using Fe_3O_4/PMG-IDA-Ni^{2+}, only a small part of BSA was removed and released from the microspheres (Figure 6, Lane 5). Therefore, the as-prepared Fe_3O_4/PVIM-2-Ni^{2+} has a much better removal ability towards high-abundant protein and exhibits better practicability in the real complex sample, which eliminates the interference of high-abundant protein BSA and facilitates the discovery of low-abundant biomarkers in the early diagnose of cancer.

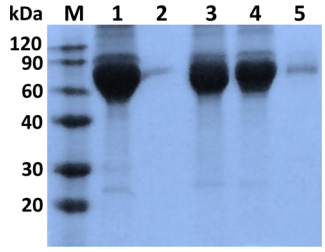

Figure 6. SDS-PAGE analysis of the removal of BSA from fetal bovine serum. Lane M: the protein molecular weight marker. Lane 1: fetal bovine serum before enrichment. Lane 2: fetal bovine serum after enrichment with Fe_3O_4/PVIM-2-Ni^{2+}. Lane 3: eluate from Fe_3O_4/PVIM-2-Ni^{2+}. Lane 4: fetal bovine serum after enrichment with Fe_3O_4/PMG-IDA-Ni^{2+}. Lane 5: eluate from Fe_3O_4/PMG-IDA-Ni^{2+}.

3.6. Sensitivity and Recyclability of the Magnetic Composite Microspheres for Histidine-rich Protein Separation. In many complex samples, histidine-rich proteins existed with quite low abundance. Therefore, it is very important for the high sensitivity of the enrichment material towards histidine-rich protein. From Figure 7a, we can find that the Fe_3O_4/PVIM-2-Ni^{2+} still effectively enrich the targeting protein even at the concentration of his-tagged protein reduced to about 40 fmoL/μL. As for the histidine-rich protein BSA, the experimental result showed that the detection limit was very low (Figure 7b). To the best of our knowledge, a detection limit as low as 40 fmoL/μL has never been reported in the previous literature, and this result hints that Fe_3O_4/PVIM-2-Ni^{2+} has the excellent ability for the enrichment of low-abundant histidine-rich proteins from complex real samples.

Besides, the recyclability and sustainability are also very important for the sake of low cost and achieving large-scale application. Herein, the recycling experiments were carried out seven times. The recyclability was evaluated by comparing the density of histidine-rich protein eluted each time with that in the first cycle on the SDS-PAGE gel. After seven cycles, the separation capability remained very well (Figure 8), which showed the excellent recyclability of the composite micro-

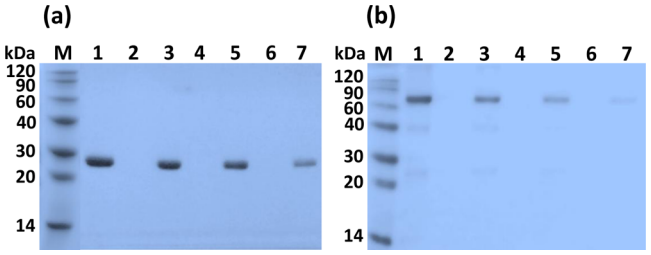

Figure 7. SDS-PAGE analysis of the enrichment of (a) his-tagged protein and (b) histidine-rich protein BSA from low concentration. Lane M: the protein molecular weight marker. Lane 1: the stock solution. (a) Lane 2, 4, 6: the stock solution diluted to 160, 80, and 40 fmoL/μL, respectively. Lane 3, 5, 7: the eluate from Fe_3O_4/PVIM-2-Ni^{2+} in the protein concentration of 160, 80, and 40 fmoL/μL, respectively. (b) Lane 2, 4, 6: the stock solution diluted to 60, 30, and 15 fmoL/μL, respectively. Lane 3, 5, 7: the eluate from Fe_3O_4/PVIM-2-Ni^{2+} in the protein concentration of 60, 30, and 15 fmoL/μL, respectively.

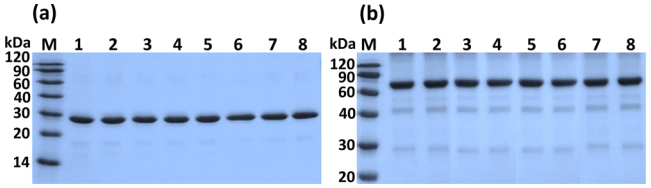

Figure 8. Recycling experiments in the separation of (a) his-tagged protein and (b) histidine-rich protein BSA. Lane M: the protein molecular weight marker. Lane 1: stock solution. Lanes 2–8: the protein released from the Fe_3O_4/PVIM-2-Ni^{2+} reused up to seven times.

spheres in the separation of his-tagged protein and BSA. It is worth mentioning that it will destroy the interaction between imidazole groups and Ni^{2+} using acidic elution solution, so the histidine-rich protein was eluted and the chelated Ni^{2+} was removed from the microspheres simultaneously. Therefore, after each elution experiment, it would take another 5 min to chelate Ni^{2+} and then used for the next recycling experiment. Exactly, it was Fe_3O_4/PVIM-2 that could be reused and recycled, while Ni^{2+} had to be chelated again in each cycle.

All of the above results displayed that the enrichment process of Fe_3O_4/PVIM-2-Ni^{2+} could be accomplished with high selectivity, excellent sensitivity, remarkable recovery, and recyclability. The isolation effect toward histidine-rich BSA is much better than the reported IDA as the affinity ligand. Considering the easy synthetic route and excellent enrichment ability toward histidine-rich proteins, the as-prepared composite microsphere is also an ideal candidate for the one-step immobilization of histidine-rich enzyme and employed for catalysis.

4. CONCLUSION

In summary, we have successfully presented a novel facile, rapid, and repeatable route for preparation of magnetic Fe_3O_4/PVIM-Ni^{2+} composite microspheres with well-defined core/shell structure, high magnetic responsiveness and pure PVIM-Ni^{2+} interfaces. To the best of our knowledge, this is the first time to utilize imidazole groups for immobilizing Ni^{2+}. Due to the strong affinity of Ni^{2+} to histidine residues, the as-prepared composite microspheres exhibit remarkable performance in enriching and separating his-tagged recombinant proteins or natural histidine-rich proteins. Furthermore, the excellent selectivity for removing of high abundant BSA from fetal bovine serum demonstrates that this kind of composite microspheres could be used in complex real samples. This material shows great potential in the biomedical applications as to facilitate the exploration of low-abundant biomarkers of disease. It also possesses a broad application prospect in the immobilization of enzymes as recyclable and active nano-biocatalysts.

■ ASSOCIATED CONTENT

Supporting Information

SEM image of Fe_3O_4 and Fe_3O_4/PVIM-2. PXRD patterns for the standard PDF card of Fe_3O_4. XPS and EDX spectra of Fe_3O_4/PVIM-Ni^{2+}. UV spectra of his-tagged protein before and after enrichment with Fe_3O_4/PVIM-Ni^{2+}. SDS-PAGE analysis of the enrichment of his-tagged protein from *E. coli* lysate using Fe_3O_4/PVIM or Fe_3O_4/PVIM-Ni^{2+}. Amino acid sequence of his-tagged protein, histidine-rich protein BSA and BHb. This material is available free of charge via the Internet at http://pubs.acs.org.

■ AUTHOR INFORMATION

Corresponding Author

*Email: ccwang@fudan.edu.cn.

Notes

The authors declare no competing financial interest.

■ ACKNOWLEDGMENTS

This work was supported by National Science and Technology Key Project of China 2012AA020204), National Science Foundation of China (Grant No. 21034003), Science and Technology Commission of Shanghai (Grant Nos. 13JC1400500 and 13520720200).

■ REFERENCES

(1) Pan, Y.; Du, X. W.; Zhao, F.; Xu, B. Magnetic Nanoparticles for the Manipulation of Proteins and Cells. *Chem. Soc. Rev.* **2012**, *41*, 2912–2942.

(2) Bao, J.; Chen, W.; Liu, T. T.; Zhu, Y. L.; Jin, P. Y.; Wang, L. Y.; Liu, J. F.; Wei, Y. G.; Li, Y. D. Bifunctional Au-Fe_3O_4 Nanoparticles for Protein Separation. *ACS Nano* **2007**, *1*, 293–298.

(3) Zhang, Y. T.; Ma, W. F.; Li, D.; Yu, M.; Guo, J.; Wang, C. C. Benzoboroxole-Functionalized Magnetic Core/Shell Microspheres for Highly Specific Enrichment of Glycoproteins under Physiological Conditions. *Small* **2014**, *10*, 1379–1386.

(4) Kim, J.; Kim, H. S.; Lee, N.; Kim, T.; Kim, H.; Yu, T.; Song, I. C.; Moon, W. K.; Hyeon, T. Multifunctional Uniform Nanoparticles Composed of a Magnetite Nanocrystal Core and a Mesoporous Silica Shell for Magnetic Resonance and Fluorescence Imaging and for Drug Delivery. *Angew. Chem. Int. Ed.* **2008**, *47*, 8438–8441.

(5) Luo, B.; Xu, S.; Luo, A.; Wang, W. R.; Wang, S. L.; Guo, J.; Lin, Y.; Zhao, D. Y.; Wang, C. C. Mesoporous Biocompatible and Acid-Degradable Magnetic Colloidal Nanocrystal Clusters with Sustainable Stability and High Hydrophobic Drug Loading Capacity. *ACS Nano* **2011**, *5*, 1428–1435.

(6) Li, D.; Tang, J.; Wei, C.; Guo, J.; Wang, S. L.; Chaudhary, D.; Wang, C. C. Doxorubicin-Conjugated Mesoporous Magnetic Colloidal Nanocrystal Clusters Stabilized by Polysaccharide as a Smart Anticancer Drug Vehicle. *Small* **2012**, *8*, 2690–2697.

(7) Wang, D. S.; He, J. B.; Rosenzweig, N.; Rosenzweig, Z. Superparamagnetic Fe_2O_3 Beads-CdSe/ZnS Quantum Dots Core-Shell Nanocomposite Particles for Cell Separation. *Nano Lett.* **2004**, *4*, 409–413.

(8) Jun, B. H.; Noh, M. S.; Kim, J.; Kim, G.; Kang, H.; Kim, M. S.; Seo, Y. T.; Baek, J.; Kim, J. H.; Park, J. Multifunctional Silver–

Embedded Magnetic Nanoparticles as SERS Nanoprobes and Their Applications. *Small* **2010**, *6*, 119−125.
(9) Gao, J. H.; Zhang, W.; Huang, P. B.; Zhang, B.; Zhang, X. X.; Xu, B. Intracellular Spatial Control of Fluorescent Magnetic Nanoparticles. *J. Am. Chem. Soc.* **2008**, *130*, 3710−3711.
(10) Kim, J.; Piao, Y.; Hyeon, T. Multifunctional Nanostructured Materials for Multimodal Imaging, and Simultaneous Imaging and Therapy. *Chem. Soc. Rev.* **2009**, *38*, 372−390.
(11) Cho, H. S.; Dong, Z. Y.; Pauletti, G. M.; Zhang, J. M.; Xu, H.; Gu, H. C.; Wang, L. M.; Ewing, R. C.; Huth, C.; Wang, F.; Shi, D. L. Fluorescent, Superparamagnetic Nanospheres for Drug Storage, Targeting, and Imaging: A Multifunctional Nanocarrier System for Cancer Diagnosis and Treatment. *ACS Nano* **2010**, *4*, 5398−5404.
(12) Song, E. Q.; Hu, J.; Wen, C. Y.; Tian, Z. Q.; Yu, X.; Zhang, Z. L.; Shi, Y. B.; Pang, D. W. Fluorescent-Magnetic-Biotargeting Multifunctional Nanobioprobes for Detecting and Isolating Multiple Types of Tumor Cells. *ACS Nano* **2011**, *5*, 761−770.
(13) Xu, S.; Ma, W. F.; You, L. J.; Li, J. M.; Guo, J.; Hu, J. J.; Wang, C. C. Toward Designer Magnetite/Polystyrene Colloidal Composite Microspheres with Controllable Nanostructures and Desirable Surface Functionalities. *Langmuir* **2012**, *28*, 3271−3278.
(14) Ohlan, A.; Singh, K.; Chandra, A.; Dhawan, S. K. Microwave Absorption Behavior of Core/Shell Structured Poly(3,4-Ethylenedioxy Thiophene)-Barium Ferrite Nanocomposites. *ACS Appl. Mater. Interfaces* **2010**, *2*, 927−933.
(15) Liu, J. Z.; Wang, W. Z.; Xie, Y. F.; Huang, Y. Y.; Liu, Y. L.; Liu, X. J.; Zhao, R.; Liu, G. Q.; Chen, Y. A Novel Polychloromethylstyrene Coated Superparamagnetic Surface Molecularly Imprinted Core/Shell Nanoparticle for Bisphenol A. *J. Mater. Chem.* **2011**, *21*, 9232−9238.
(16) Li, G. L.; Shi, Q.; Yuan, S. J.; Neoh, K. G.; Kang, E. T.; Yang, X. L. Alternating Silica/Polymer Multilayer Hybrid Microspheres Templates for Double-Shelled Polymer and Inorganic Hollow Microstructures. *Chem. Mater.* **2010**, *22*, 1309−1317.
(17) Ma, W. F.; Zhang, Y.; Li, L. L.; Zhang, Y. T.; Yu, M.; Guo, J.; Lu, H. J.; Wang, C. C. Ti^{4+}-Immobilized Magnetic Composite Microspheres for Highly Selective Enrichment of Phosphopeptides. *Adv. Funct. Mater.* **2013**, *23*, 107−115.
(18) Jin, S.; Pan, Y. J.; Wang, C. C. Reflux Precipitation Polymerization: A New Technology for Preparation of Monodisperse Polymer Nanohydrogels. *Acta Chim. Sinica* **2013**, *71*, 1500−1504.
(19) Gaberc-Porekar, V.; Menart, V. Potential for Using Histidine Tags in Purification of Proteins at Large Scale. *Chem. Eng. Technol.* **2005**, *28*, 1306−1314.
(20) Lata, S.; Reichel, A.; Brock, R.; Tampe, R.; Piehler, J. High-Affinity Adaptors for Switchable Recognition of Histidine-Tagged Proteins. *J. Am. Chem. Soc.* **2005**, *127*, 10205−10215.
(21) Kim, J.; Piao, Y.; Lee, N.; Park, Y. I.; Lee, I. H.; Lee, J. H.; Paik, S. R.; Hyeon, T. Magnetic Nanocomposite Spheres Decorated with NiO Nanoparticles for a Magnetically Recyclable Protein Separation System. *Adv. Mater.* **2010**, *22*, 57−60.
(22) Wang, W.; Wang, C.; Li, Z. Facile Fabrication of Recyclable and Active Nanobiocatalyst: Purification and Immobilization of Enzyme in One Pot with Ni-NTA Functionalized Magnetic Nanoparticle. *Chem. Commun.* **2011**, *47*, 8115−8117.
(23) Shukoor, M. I.; Natalio, F.; Therese, H. A.; Tahir, M. N.; Ksenofontov, V.; Panthofer, M.; Eberhardt, M.; Theato, P.; Schroder, HC.; Müller, WEG.; Tremel, W. Fabrication of a Silica Coating on Magnetic γ-Fe_2O_3 Nanoparticles by an Immobilized Enzyme. *Chem. Mater.* **2008**, *20*, 3567−3573.
(24) Shao, M. F.; Ning, F. Y.; Zhao, J. W.; Wei, M.; Evans, D. G.; Duan, X. Preparation of Fe_3O_4@SiO_2@Layered Double Hydroxide Core-Shell Microspheres for Magnetic Separation of Proteins. *J. Am. Chem. Soc.* **2012**, *134*, 1071−1077.
(25) Li, Y. C.; Lin, Y. S.; Tsai, P. J.; Chen, C. T.; Chen, W. Y.; Chen, Y. C. Nitrilotriacetic Acid-Coated Magnetic Nanoparticles as Affinity Probes for Enrichment of Histidine-Tagged Proteins and Phosphorylated Peptides. *Anal. Chem.* **2007**, *79*, 7519−7525.
(26) Liu, Z.; Li, M.; Yang, X. J.; Yin, M. L.; Ren, J. S.; Qu, X. G. The Use of Multifunctional Magnetic Mesoporous Core/Shell Heteronanostructures in a Biomolecule Separation System. *Biomaterials* **2011**, *32*, 4683−4690.
(27) Fang, W. J.; Chen, X. L.; Zheng, N. F. Superparamagnetic Core/Shell Polymer Particles for Efficient Purification of His-Tagged Proteins. *J. Mater. Chem.* **2010**, *20*, 8624−8630.
(28) Xu, F.; Geiger, J. H.; Baker, G. L.; Bruening, M. L. Polymer Brush-Modified Magnetic Nanoparticles for His-Tagged Protein Purification. *Langmuir* **2011**, *27*, 3106−3112.
(29) Zhen, G. L.; Falconnet, D.; Kuennemann, E.; Voros, J.; Spencer, N. D.; Textor, M.; Zurcher, S. Nitrilotriacetic Acid Functionalized Graft Copolymers: A Polymeric Interface for Selective and Reversible Binding of Histidine-Tagged Proteins. *Adv. Funct. Mater.* **2006**, *16*, 243−251.
(30) Zhang, M.; He, X. W.; Chen, L. X.; Zhang, Y. K. Preparation of IDA-Cu Functionalized Core-Satellite Fe_3O_4/Polydopamine/Au Magnetic Nanocomposites and Their Application for Depletion of Abundant Protein in Bovine Blood. *J. Mater. Chem.* **2010**, *20*, 10696−10704.
(31) Xu, C.; Xu, K.; Gu, H.; Zhong, X.; Guo, Z.; Zheng, R.; Zhang, X.; Xu, B. Nitrilotriacetic Acid-Modified Magnetic Nanoparticles as a General Agent to Bind Histidine-Tagged Proteins. *J. Am. Chem. Soc.* **2004**, *126*, 3392−3393.
(32) Xu, C.; Xu, K.; Gu, H.; Zheng, R.; Liu, H.; Zhang, X.; Guo, Z.; Xu, B. Dopamine as a Robust Anchor to Immobilize Functional Molecules on the Iron Oxide Shell of Magnetic Nanoparticles. *J. Am. Chem. Soc.* **2004**, *126*, 9938−9939.
(33) Jian, G. Q.; Liu, Y. X.; He, X. W.; Chen, L. X.; Zhang, Y. K. Click Chemistry: A New Facile and Efficient Strategy for the Preparation of Fe_3O_4 Nanoparticles Covalently Functionalized With IDA-Cu and Their Application in the Depletion of Abundant Protein in Blood Samples. *Nanoscale* **2012**, *4*, 6336−6342.
(34) Cao, J. L.; Zhang, X. H.; He, X. W.; Chen, L. X.; Zhang, Y. K. Facile Synthesis of a Ni (ii)-Immobilized Core-Shell Magnetic Nanocomposite as an Efficient Affinity Adsorbent for the Depletion of Abundant Proteins from Bovine Blood. *J. Mater. Chem. B* **2013**, *1*, 3625−3632.
(35) Zhang, Y. T.; Li, L. L.; Ma, W. F.; Zhang, Y.; Yu, M.; Guo, J.; Wang, C. C. Two-in-One Strategy for Effective Enrichment of Phosphopeptides Using Magnetic Mesoporous γ-Fe_2O_3 Nanocrystal Clusters. *ACS Appl. Mater. Interfaces* **2013**, *5*, 614−621.
(36) Zhang, Y. T.; Yang, Y. K.; Ma, W. F.; Guo, J.; Lin, Y.; Wang, C. C. Uniform Magnetic Core/Shell Microspheres Functionalized with Ni^{2+}-Iminodiacetic Acid for One Step Purification and Immobilization of His-Tagged Enzymes. *ACS Appl. Mater. Interfaces* **2013**, *5*, 2626−2633.